# Multifunctional PV-based EV System under Distorted Grid Condition using Modified-STF

Sudarshan Swain, Aman Dudeja and Abhisek Parida

***Abstract*—In this paper, we analyse the performance of a multifunctional PV-based EV system under distorted grid condition. In this work, a Modified Self Tuning Filter (MSTF) is proposed to improve the power quality. The control scheme adapted makes the PV-based EV system multifunctional as it extracts maximum solar power, which is then used to charge the EV battery at rated power and also supply power to the non linear load. The additional extracted PV power is then injected into the grid. The load current harmonics are mitigated to maintain sinusoidal grid current. The sinusoidal grid current obtained is in phase with the PCC voltage to ensure unity power factor operation. The grid current settles to a THD value, well under the limits of grid codes specified by IEEE 519. The proposed scheme is analysed under steady-state as well as in dynamic conditions in MATLAB. The results obtained show that the proposed MSTF-PI control scheme maintains efficient power flow during steady-state as well as dynamic conditions thereby improving the power quality.**

***Index Terms*—PV array, Electric Vehicle(EV), Power Quality, Harmonic mitigation, MSTF**

## I. Introduction

Over the the past few years, there has been a significant shift towards the use of renewable energy and electric vehicle systems. It is anticipated that almost all the vehicles would be electric by the year 2030 based on the various positive impacts of electrification in various sectors [1]. Conventionally, charging of EV's require large amount of electrical energy to be drawn from grid or some coal/gas based power plant [2]. An analysis over impact of uncoordinated charging of the EV from grid concludes that it leads to overloading of the grid, thereby introducing the voltage harmonics and fluctuation as well as increasing the losses [4]. A coordinated control scheme is therefore required and can be implemented by charging the EV from a renewable source such as the PV instead of grid. In the present scenario, 99% of the PV systems are in grid connected mode [3]. The primary reason for this being the storage of energy in isolated mode does not reap as much benefits on an individual level as in a grid connected configuration where one can get economic benefits as well in form of reduced electricity bill. It also prevents the overloading of grid in the cases of high demand. Not only can PV be used to feed load but it can be very useful in charging an EV battery. [5] demonstrated that in a coordinated control scheme, reactive power removal from EVs helped manage grid constraints like voltage fluctuations and undervoltage. It also helped in mitigating issues caused by solar irradiance by absorbing the power fluctuations of the PV array [6]. A PV based system therefore can be used to charge the EV battery, take care of house load demands and supply any excess power into the grid. This configuration with a PV-based EV charging in presence of grid and load, therefore, presents a practical and viable solution moving forward. However there are few issues that need to be addressed for this configuration. A non linear load draws non sinusoidal current from the grid thereby degrading the grid and resulting in poor power quality [7]. Varying temperature and irradiance also have an impact on the behaviour of the system. An efficient approach is therefore required to maintain power quality. This can be done by using an active power filter. A grid integrated PV system is considered to have a high efficiency if unity power factor is achieved and if the grid current is maintained sinusoidal [8]. To achieve this it is important to estimate the active component of load current and extract maximum power from the PV array. This depends not only on the intrinsic factors of the PV module used but also on external factors such as temperature and irradiance.

There are many efficient algorithms in the literature for maximum power point estimation such as Perturb and Observe (PnO), Incremental Conductance (InC), double integral sliding mode etc. [9-10]. PnO works by updating the operating point based on the power versus voltage characteristics. However, the drawback is in form of the undesired oscillations at the operating point. Whereas InC algorithm works by tracking the MPP such that sum of conductance and incremental conductance is minimum [11]. The rapidly increasing non linear loads and power electronic switching is making the PV integration more challenging, one major issue being the fundamental component extraction. To address this, several types of control schemes have been proposed in the literature such as: synchronous reference frame theory [12], fuzzy logic control [13], adaptive filtering control [14], Kalman filtering techniques [15], instantaeneous reactive power theory [16] and ILST algorithm [17]. However, the the above algorithms have few drawbacks such as high complexity, inter harmonics at DC input signal, higher response time, zero DC offset rejection, computational burden and inadequacy under distorted grid conditions. A Self Tuning Filter (STF) is proposed in [18] which has better response time and reduced area requirement. However, the STF algorithm has a drawback of less efficient performance under dynamic conditions due to the abc to $\alpha$-$\beta$ transformation. An Enhanced Self Tuning Filter (ESTF) with active power filters is proposed in [19] for control of a single phase dynamic voltage regulator. ESTF is a three input three output system which provides improved performance over other algorithms. However, ESTF uses two cascaded units of the actual filter. The proposed Modified STF (MSTF) algorithm has a single unit and is an improved version of the

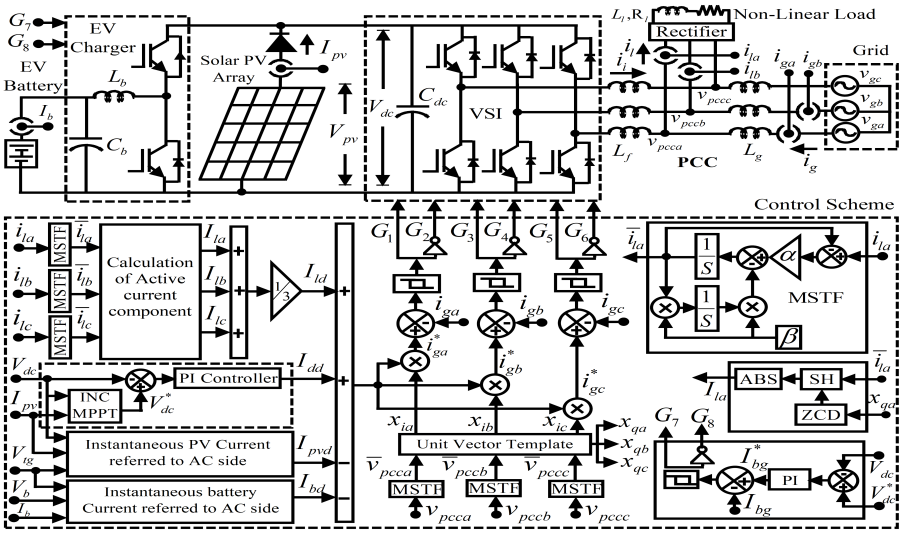


Fig. 1. System Overview

conventional STF. MSTF is a single stage self tuning filter which provides even better filtering and response time results than the ESTF. It also has higher accuracy, less complexity making it easy to implement. The improved performance of MSTF over some of the existing filtering techniques makes it a suitable choice, therefore, we intend to extend the application of MSTF by proposing a MSTF-PI control scheme for the PV-based EV system.

In this work, the performance of the proposed MSTF-PI control scheme is analysed for PV-based EV system under distorted grid conditions. Performance analysis is carried out during steady-state as well as dynamic conditions. The MSTF serves two main objectives: to extract unit in phase and quadrature templates from PCC voltages and to extract the fundamental load current component. The control is designed to support unidirectional EV charging and smart power distribution among grid, EV, load and PV, and to maintain power quality in grid by mitigating the current harmonics. Another distinct feature of this scheme is that the MPPT algorithm has been implemented without the use of DC-DC converter to reduce circuit complexity while maintaing efficiency. The objectives of this paper are as follows:

- Design a MSTF-PI control scheme to provide fast and accurate estimation of unit templates from the PCC voltage and the load current.
- Extracting Maximum PV power from the PV arrays
- Charging the battery at the rated voltage and power by designing a DC-DC converter control
- Designing an effective power flow scheme for the system.

## II. System Overview

The proposed system configuration is shown in Fig. 1. An IGBT based shunt voltage source converter(VSC) is used. A three phase rectifier circuit with RL branch is used as non linear load. PV array is connected across the DC Link capacitor. EV battery is connected across the DC link via a DC-DC converter which operates in buck mode. A maximum power point algorithm has been used to extract maximum power from the PV array. Interfacing inductors between the VSC and grid have been used to reduce the harmonics in the grid current and preserve it's sinusoidal nature. The entire sytem was implemented in MATLAB/Simulink and the results for the same is shown in the results section.

## III. Control Scheme

The primary purpose of the proposed MSTF-PI control is to make efficient energy utilization in the PV-based EV system and also improve the overall power quality. PV array, EV battery and grids are synchronised for an efficient power flow under dynamic conditions. An InC based MPPT algorithm has been used to extract maximum PV power. The control scheme is divided into two parts which are discussed as:

### A. DC-DC Converter Control

The PV array supplies the generated power to the EV battery via a DC-DC Converter which operates in buck mode to step down the voltage to the rated battery voltage specification. Since it draws power from the PV array, it decreases the DC link voltage across the DC link capacitor. Hence, another role of this control is to maintain the DC link voltage. To generate the reference battery current we make use of the reference DC link voltage generated by MPPT. This $V_{dc}^{*}$ is compared with the actual $V_{dc}$ and the error is sent to a PI controller. The discrete domain equation is given as in (1),

$$I_{bg}^{*}(k) = k_{pbg}[v_{dce}(k) - v_{dce}(k-1)] + k_{ibg}v_{dce}(k) + I_{bg}(k-1) \quad (1)$$

Where, $v_{dce}$ is the error voltage of $V_{dc}^{*}$ and $V_{dc}$. $k_{pbg}$ and $k_{ibg}$ are the proportional and integral gain constants of the controller. This reference battery current along with the measured battery current is sent to the the hysteresis current controller to generate the gating pulses G7 and G8 as shown in Fig. 1.

### B. Voltage Source Converter Control

The VSC control scheme has been shown in Fig. 1. The following quantities are used for control: the power being generated by PV array ($P_{pv}$), the sensed DC link voltage

across $C_{dc}$ ($V_{dc}$), the reference DC link voltage generated by MPPT ($V_{dc}^*$), the sensed PCC voltages ($v_{pcca}$,$v_{pccb}$,$v_{pccc}$), the sensed load currents ($i_{la}$,$i_{lb}$,$i_{lc}$),the grid currents ($i_{ga}$,$i_{gb}$,$i_{gc}$) and the battery parameters ($I_{bg}$,$P_b$). The control is based on estimating the reference grid currents ($i_{ga}^*$,$i_{gb}^*$,$i_{gc}^*$) via a unit template generation control. The reference grid current is estimated by product of fundamental active component of estimated current ($I_{net}$) with the unit in phase templates. The sensed PCC voltages are sensed and are filtered out using a modified self tuning filter to remove any distortions present. The filtered PCC voltages ($\bar{v}_{pcca}$,$\bar{v}_{pccb}$,$\bar{v}_{pccc}$) are then used to estimate unit in phase and quadrature phase templates. The terminal voltage amplitude is estimated as follows,

$$V_{tg} = \sqrt{\frac{2}{3}(\bar{v}_{pcca}^2 + \bar{v}_{pccb}^2 + \bar{v}_{pccc}^2)} \tag{2}$$

In phase unit templates are generated by the following equations,

$$x_{ia} = \frac{\bar{v}_{pcca}}{V_{tg}}, x_{ib} = \frac{\bar{v}_{pccb}}{V_{tg}}, x_{ic} = \frac{\bar{v}_{pccc}}{V_{tg}} \tag{3}$$

Similarly, quadrature phase unit templates are generated by,

$$x_{qa} = \frac{-x_{ib}}{\sqrt{3}} + \frac{x_{ic}}{\sqrt{3}}, x_{qb} = \frac{\sqrt{3}x_{ia}}{2} + \frac{x_{ib} - x_{ic}}{2\sqrt{3}}, \quad x_{qc} = \frac{-\sqrt{3}x_{ia}}{2} + \frac{x_{ib} - x_{ic}}{2\sqrt{3}} \tag{4}$$

These unit templates obtained in (3) and (4) are used for active reference grid current estimation that are synchronous with the grid voltage. The current magnitude contributed by load side is calculated by first estimating the fundamental component of load current using the MSTF, and, then extracted using sample hold of load current and zero crossing detection with quadrature unit templates generated in (4) to generate the fundamental components of load currents: $I_{la}$, $I_{lb}$, $I_{lc}$. The net load current contribution is given by,

$$I_{ld} = \frac{I_{la} + I_{lb} + I_{lc}}{3} \tag{5}$$

The transfer function of the MSTF is given by (6). where $\alpha$ is the gain of transfer function and $\beta$ is the cutoff frequency in rad/sec.

$$G(s) = \frac{\alpha s}{(s^2 + \alpha s + \beta^2)} \tag{6}$$

Bode plot response of the filter for in-phase signal is also shown in Fig. 2. Due to zero gain at $s$ = 0, MSTF nullifies the DC offset and provides good filtering performance at the rated supply frequency. The poles obtained from transfer function for the values of $\alpha$ and $\beta$ given in Table I are $s$ = -5 $\pm$ 314.12$i$. Since both poles lie in the left half $s$ plane, MSTF is stable. The current component required to maintain DC link voltage is calculated using a PI controller as given in (7) which is fed the error voltage at DC link $v_{dce}$ to generate the required current $I_{dd}$.

$$I_{dd}(k) = k_{pdc}[v_{dce}(k) - v_{dce}(k-1)] + k_{idc}v_{dce}(k) + I_{dd}(k-1) \tag{7}$$

$V_{dc}^*$ is calculated via the MPPT algorithm. In this work we have used the incremental conductance algorithm. MPPT control estimates the voltage across PV that generates maximum power. In this algorithm the slope of $P_{pv}$ vs $V_{pv}$ curve is

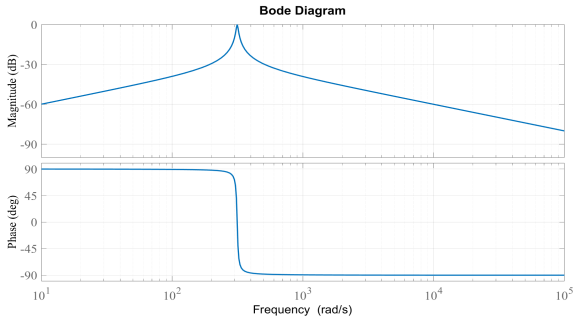


Fig. 2. Bode Plot Response of Self Tuning Filter

measured and operating point is moved by a small increments after every iteration until the slope achieved is zero. The operating point is tracked such that the sum of conductance and incremental conductance is minimum. It effectively tracks the maximum power point under dynamic conditions such as varying temperatures and irradiance as well. The PV current $I_{pv}$ and the DC link voltage $V_{dc}$ are given as inputs to generate a reference maximum power operating voltage $V_{dc}^*$. The battery current component referred to grid side ($I_{bd}$) is given by,

$$I_{bd} = \frac{2 \times P_b}{V_{tg}} \tag{8}$$

Similarly, the PV array current component referred to grid side ($I_{pvd}$) is given by,

$$I_{pvd} = \frac{2 \times P_{pv}}{V_{tg}} \tag{9}$$

Now, the net reference current magnitude is calculated from the equation,

$$I_{net} = I_{dd} + I_{ld} - I_{bd} - I_{pvd} \tag{10}$$

From $I_{net}$ and the in phase unit templates we can get the reference grid current by,

$$i_{ga}^* = I_{net} \times x_{ia}, i_{gb}^* = I_{net} \times x_{ib}, i_{gc}^* = I_{net} \times x_{ic} \tag{11}$$

These reference currents along with the sensed grid currents are then passed into the hysteresis controller to generate the gating pulses G1 to G6.

## IV. Result and Discussion

The system has been implemented in MATLAB and Simulink. A distorted grid has been considered in all simulations. The grid contains $3^{rd}$ and $5^{th}$ harmonics with an amplitude of 0.02 and 0.03 per unit respectively. A 10 kW (at 298 K) rated PV module has been selected. The EV battery power is rated at 2.5 kW with a rating of 310 V and 10 Ah. A non linear load rated at 1.45 kW is considered. Under nominal conditions (298 K and 1000 W/$m^2$ irradiance), the DC link voltage is 655 V. The dynamic response in case of varying parameters has also been shown in further sections. The control is initialised at 0.6 sec. The various parameters for simulations have been shown in Table I. The PV array parameters have been taken from [17].

### A. Steady-State Performance

The steady-state performance analysis is simulated at a temperature of 298 K with an irradiance to the PV of 1000 W/$m^2$. The battery starts charging and then operates at its nominal voltage and current values of 310 V and 7.5 A respectively. The negative value of current indicates the power absorbing nature and thus charging state. Fig. 3(a-c) show the

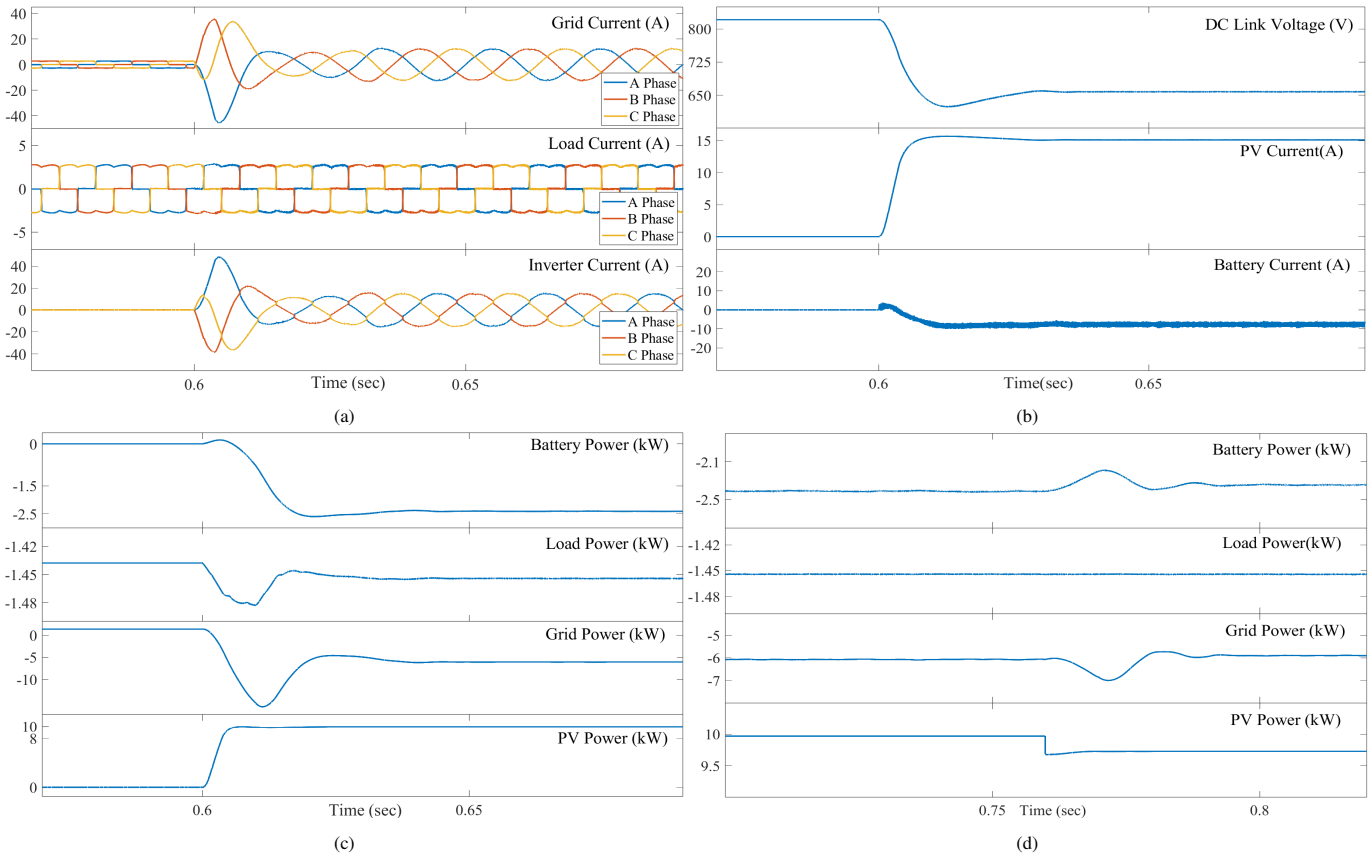


Fig. 3. (a) AC side currents under steady-state conditions, (b) DC side currents under steady-state conditions, (c) Power flow under steady-state conditions, (d) Power Flow under temperature variation

TABLE I
PARAMETERS FOR SIMULATION STUDY

| Symbols | Parameters | Values |
|---|---|---|
| $v_g$ | Supply Voltage | 400 V |
| $f_g$ | PCC Voltage | 50 Hz |
| $L_s$ | Supply Inductance | 0.5 mH |
| $L_f$ | Interfacing Inductance | 10 mH, |
| $R_l$ | Load Resistance | 200 Ω, |
| $L_l$ | Load Inductance | 25 mH, |
| $C_{dc}$ | DC-link Capacitance | 800 µF |
| $L_b$ | Battery interfaced Inductance | 2 mH, |
| $C_b$ | Battery interfaced Capacitance | 1 mF |
| $k_{pdc}$, $k_{idc}$ | Proportional and Integral Gain | 0.3, 0.4 |
| $k_{pbg}$, $k_{ibg}$ | Proportional and Integral Gain | 0.4, 0.6 |
| $\alpha$ | STF Gain | 10 |
| $\beta$ | Cut-off Frequency | 314.16 rad/sec |
| $V_{br}$ | Rated Voltage | 310 V |
| $C_r$ | Rated Capacity | 10Ah |

response of the system from $t$ = 0.55 sec to $t$ = 0.7 sec under steady-state conditions. Fig. 3(a) shows the AC side currents of the system which includes the load current, inverter current and grid current response with respect to time. The THD of grid current was recorded as 3.1% which is well under the IEEE limits with the use of the analysed MSTF, thus improving the power quality of the grid. Fig. 3(b) gives the DC Link voltage response as well as the battery and PV currents. DC link voltage reaches it's steady state value of 655 V at 0.63 sec. PV current and battery current also enter their steady state at 0.62 sec. The power flow of the complete system can be seen in Fig. 3(c). The equation governing the power flow is given by eq. (12). It follows the universal rule that power delivered at one part of system is absorbed in another part. The convention used here is that positive power means power is being delivered by the module and negative power means power is being absorbed by the module. Grid power is negative if PV power is able to meet the battery and load requirements indicating the remaining power to be fed to the grid. Positive grid power indicates vice versa.

$$P_{pv} - P_b - P_{load} \pm P_{grid} - P_{losses} = 0 \qquad (12)$$

We can observe that the PV is delivering 10 kW power of which EV battery is absorbing 2.41 kW, Load absorbs 1.45 kW and remaining 6.1 kW of power is injected into the grid. Therefore, from (12) we can observe that out of the 10 kW power generated by PV, 9.96 kW is supplied to the grid,load and the battery. Remaining 0.04 kW accounts for the various kinds of losses combined which includes losses through passive elements and inverter losses.

### *B. Performance under varying Temperature*

Temperature variation has an inversely proportional impact on the power a PV array generates. We increased the temperature from 298 K to 303 K at $t$ = 0.767 sec, all other parameters are same as previous section. The following results were recorded. Fig. 4(a) shows the dynamic response of DC link voltage, PV current, load current and grid current under

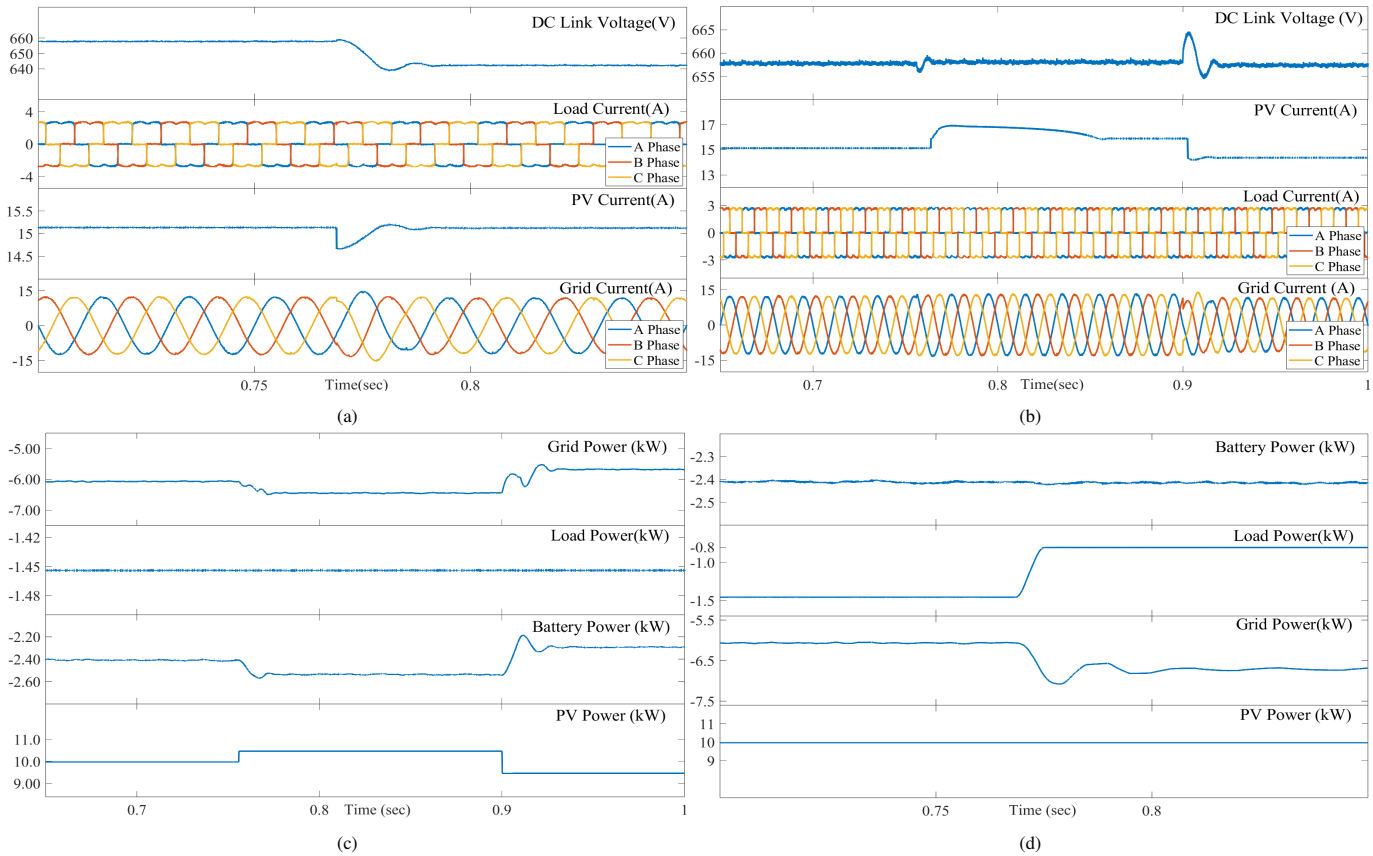


Fig. 4. (a) Performance under temperature variation, (b) Performance under irradiance variation, (c) Power flow under irradiance variation, (d) Power flow under load fault

temperature variation. It can be inferred that for temperature variations, grid current,PV current and DC-link voltage quickly stabilise themselves and MPPT finds the new operating point to supply maximum power, here being 643 V. Fig. 3(d). shows the power flow in the system pre and post temperature variation. The power generated by PV decreases to 9.725 kW. The power delivered to grid also thereby decreases to 5.9 kW. The battery power absorbed reduces to 2.35 kW. The load power remains same. The power flow equation can again be verified by putting these values in (12). Grid current THD is recorded to be 3.1%. Therefore the system proves its efficient performance under dynamic temperature conditions under distorted grid.

### C. Performance under varying Irradiance

Fig. 4(b-c). show the complete dynamic performance characteristics of the system under varying irradiance. Irradiance and temperature share a directly proportional relationship. Initially irradiance is 1000 W/$m^2$. We analyse the the behaviour of the system under the following dynamic irradiance conditions: at $t$ = 0.76 sec irradiance is increased to 1050 W/$m^2$ and at $t$ = 0.9 sec it is decreased to 950 W/$m^2$. From the DC link voltage characteristics in Fig. 4(b), we can infer that DC link voltage stabilises itself rapidly. At 0.76 sec, DC link voltage is updated and stabilises till 0.77 sec. The second higher variation in irradiation which happens at 0.9 sec achieves stability by 0.92 sec. We can also observe from Fig. 4(c) that at 0.76 sec, PV power delivered increases to 10.47 kW, battery power taken in to 2.54 kW and power given back to grid to 6.45 kW. Load power remains same at 1.45 kW. Equation (12) is satisfied in this case. At 0.9 sec, the irradiance drops from 1050 W/$m^2$ to 950 W/$m^2$. The powers recorded are as follows, PV power generated is 9.46 kW, battery power absorbed is 2.29 kW, power injected in grid is 5.68 kW and load power is 1.45 kW. Grid THD is recorded at 3.2% and both grid and PV currents are rapidly stabilised by the control. Thus, the system is effective in improving and sustaining the power quality of grid under dynamic irradiance conditions as well in a distorted grid.

### D. Performance under Load fault

Load faults can be very useful in determining the efficiency of a system under dynamic conditions. Here, we have simulated load fault by disconnecting phase B to the load at 0.76 seconds. This can lead to sudden rise in 3rd harmonic in the load side as compared to before the fault. Fig. 4(d) shows the power flow under load fault. At 0.76 seconds as phase B to load is disconnected, we can note some drop in load power absorbed from 1.45 kW to 0.8 kW. But since PV and battery power are unaffected by a load fault, the drop in load power absorption is compensated by increase in grid power absorption from 6.1 kW to 6.75 kW. The power flow equation is satisfied. Grid current and load current response are given in Fig. 5(a). Grid current THD recorded a slight increase to 3.8%. Battery current response remains unaffected. However PV current Fig. 5(b) showed small oscillations after a load

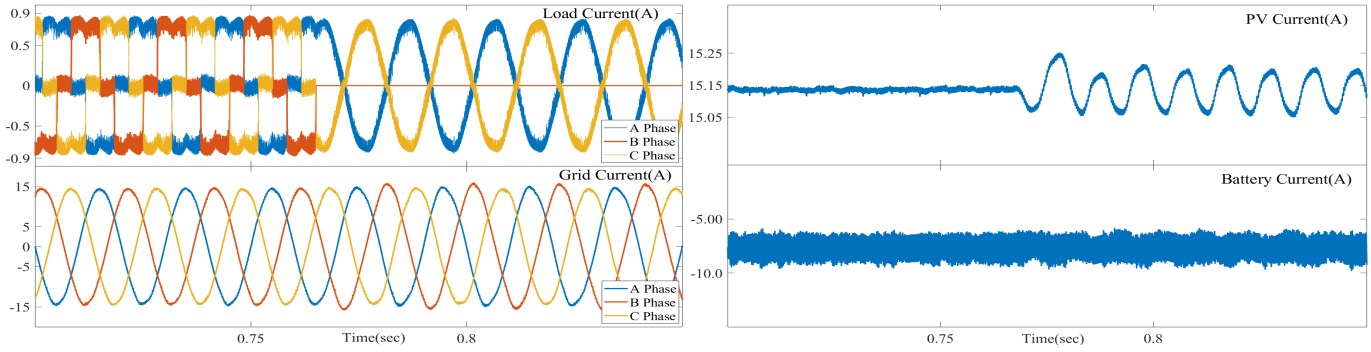


(a) (b)

Fig. 5. (a) Load and Grid currents under load fault, (b) PV and Battery currents under load fault

fault, although this did not impact the overall performance of the system. Hence, grid current THD is maintained under IEEE limits thereby maintaining a good power quality and a smart power flow operation under this dynamic scenario.

## V. Conclusion

A new modified self tuning filter based EV charging system using solar power in grid connected mode is implemented in MATLAB/Simulink. The performance analysis of the scheme is carried out under dynamic conditions such as temperature irradiance variation and load faults. Voltage source control is based on active power control using reference grid current estimation. This was done by extracting unit in phase and quadrature phase templates using the modified self tuning filter. MSTF has shown it's excellent efficiency by enabling the control to mitigate the current harmonics under distorted grid and various dynamic conditions. A DC-DC buck converter is used to supply the EV battery at rated power. EV Battery charges efficiently at nominal rate in this scheme. The model is simple to implement and provides an efficient solution to multiple problems such as renewable energy as an alternative to home power demand as well as an Electric vehicle charging source. Simulations of the proposed scheme show an effective control of the grid current THD within 3.8% in load fault scenario and within 3.2% for all the other conditions considered, thus helping improve the power quality and ensuring the stable operation of power system. Hence, the results obtained validate the efficiency of the model.

## References


[1] N. Abhyankar, A.R. Gopal, C. Sheppard, W.Y. Park, A.A. Phadke, "All electric passenger vehicle sales in India by 2030: value proposition to electric utilities, government, and vehicle owners" Lawrence Berkeley National Laboratory, 2017, LBNL Report #: LBNL-1007121.

[2] D. Manz, R. Walling, N. Miller, B. LaRose, R. D'Aquila and B. Daryanian, "The Grid of the Future: Ten Trends That Will Shape the Grid Over the Next Decade," IEEE Power and Energy Magazine, vol. 12, no. 3, pp. 26-36, 2014.

[3] S. Kouro, J. I. Leon, D. Vinnikov and L. G. Franquelo, "Grid-Connected Photovoltaic Systems: An Overview of Recent Research and Emerging PV Converter Technology," IEEE Industrial Electronics Magazine, vol. 9, no. 1, pp. 47-61, 2015.

[4] K. Clement-Nyns, E. Haesen and J. Driesen, "The Impact of Charging Plug-In Hybrid Electric Vehicles on a Residential Distribution Grid," IEEE Trans. on Power Systems, vol. 25, no. 1, pp. 371-380, 2010.

[5] J. Wang, G. R. Bharati, S. Paudyal, O. Ceylan, B. P. Bhattarai and K. S. Myers, "Coordinated Electric Vehicle Charging with Reactive Power Support to Distribution Grids,"IEEE Transactions on Industrial Informatics, vol. 15, no. 1, pp. 54-63,2019.

[6] J. Traube, F. Lu, D. Maksimovic, J. Mossoba, M. Kromer, P. Faill, Stan Katz, Bogdan Borowy, Steve Nichols, L. Casey, ,"Mitigation of Solar Irradiance Intermittency in Photovoltaic Power Systems With Integrated Electric-Vehicle Charging Functionality," IEEE Transactions on Power Electronics, vol. 28, no. 6, pp. 3058-3067, 2013.

[7] K. Nikum, R. Saxena and A. Wagh, "Effect on power quality by large penetration of household non linear load," IEEE 1st Int. Conference on Power Electronics, ICPEICES, Delhi, India, pp. 1-5, 2016.

[8] S. Swain and B. Subudhi, "A new grid synchronisation scheme for a three-phase pv system using self-tuning filtering approach," IET Generation, Transmission and Dist., vol. 11, no. 14, p. 3557–3567, 2017.

[9] B. Subudhi and R. Pradhan, "A Comparative Study on Maximum Power Point Tracking Techniques for Photovoltaic Power Systems," IEEE Transactions on Sustainable Energy, vol. 4, no. 1, pp. 89-98, Jan. 2013.

[10] T. Esram and P. L. Chapman, "Comparison of Photovoltaic Array Maximum Power Point Tracking Techniques," IEEE Transactions on Energy Conversion, vol. 22, no. 2, pp. 439-449, 2007.

[11] R. Faraji, A. Rouholamini, H. R. Naji, R. Fadaeinedjad and M. R. Chavoshian, "FPGA-based real time incremental conductance maximum power point tracking controller for photovoltaic systems",IET Power Electronics, vol. 7, no. 5, pp. 1294-1304, 2014.

[12] F. Gonzalez-Espin, G. Garcera, I. Patrao, et al.,"An adaptive control system for three-phase photovoltaic inverters working in a polluted and variable frequency electric grid," IEEE Tran. Power Electron., vol 27, no. 10, pp. 4248–4261, 2012.

[13] M. A. Hannan, Z. A. Ghani, A. Mohamed and M. N. Uddin, "Real-Time Testing of a Fuzzy-Logic-Controller-Based Grid-Connected Photovoltaic Inverter System," IEEE Transactions on Industry Applications, vol. 51, no. 6, pp. 4775-4784, 2015.

[14] H. M. Hasanien, "An Adaptive Control Strategy for Low Voltage Ride Through Capability Enhancement of Grid-Connected Photovoltaic Power Plants," IEEE Transactions on Power Systems, vol. 31, no. 4, pp. 3230-3237, 2016.

[15] M. S. Reza, M. Ciobotaru and V. G. Agelidis, "Instantaneous power quality analysis using frequency adaptive kalman filter technique," Proceedings of The 7th International Power Electronics and Motion Control Conference, Harbin, China, pp. 81-87, 2012.

[16] B. Singh, D. T. Shahani and A. K. Verma, "IRPT based control of a 50 kw grid interfaced solar photovoltaic power generating system with power quality improvement," 4th IEEE International Symposium on PEDG, Rogers, USA, pp. 1-8, 2013.

[17] B. Singh, C. Jain, and S. Goel, "Ilst control algorithm of single-stage dual purpose grid connected solar pv system," IEEE Transactions on Power Electronics, vol. 29, no. 10, pp. 5347–5357, 2014.

[18] S. Biricik, S. Redif, C. Ozerdem, S.K. Khadem, M. Basu, "Real-time control of shunt active power filter under distorted grid voltage and unbalanced load condition using self-tuning filter," IET Power Electron, Vol. 7, no. 7, pp. 1895–1905, 2014.

[19] H. Ahmed, S. Biricik, Hasan Komurcugil, S.B. Elghali, M. Benbouzid, "Enhanced frequency-adaptive self-tuning filter-based continuous terminal sliding mode control of single-phase dynamic voltage restorer," Control Engineering Practice, Vol. 128, ISSN 0967-0661, 2022.